Jurnal Teknologi

Full paper

Image Reconstruction Methods for Ultrasonic Transmission Mode Tomography in Bubbly Flow Regime

Mahdi Faramarzi, Sallehuddin Ibrahim*, Mohd Amri Md Yunus, Jaysuman Pusppanathan

Control and Instrumentation Department, Faculty of Electrical Engineering, Universiti Teknologi Malaysia, 81310, UTM Johor Bahru, Johor, Malaysia

*Corresponding author: salleh@fke.utm.my

Article history

Received :5 February 2014
Received in revised form :
7 April 2014
Accepted :20 May 2014

Graphical abstract

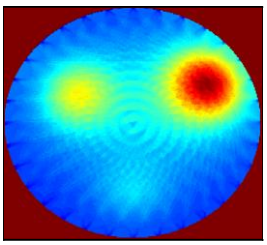

Abstract

Image reconstruction from projections plays an important role in monitoring flow regimes by ultrasonic transmission mode tomography (UTMT) system. Fast and more accurate methods are necessary in case of on-line process e.g. bubbly flow regimes. In this work, analytical image reconstruction methods such as linear back projection (LBP), filter back projection (FBP) and convolution back projection (CBP) in bubbly flow regime is investigated and found that CBP is superior to other methods. Furthermore, different filters were applied to CBP to investigate the image quality improvement. Among different types of filters for CBP method, Ram-lack outperforms the others for UTMT. The peak signal to noise ratio (PSNR) of reconstructed images in this particular experiment was improved using Ram-lack in noiseless data.

Keywords: Analytical image reconstruction; LBP; CBP; ultrasonic transmission mode tomography

1.0 INTRODUCTION

Ultrasonic tomography (UT) system was introduced as a non-intrusive and non-invasive testing tool for industrial process monitoring [1]. The hardware drawbacks of UT systems are their physical size limitations of sensors and sound limitations in materials [2]. The first reduces the number of sensors mounted around the peripheral of pipe while the second limitation decreases the quality of reconstructed image in motion flow and also increase the time of data gathering from sensors. During last decades there are many attempts have been done to improve the image quality and increase the speed of monitoring by development of the ultrasonic system hardware [3-9]. Up to now, different types of UT system configurations with different excitation frequencies have been studied to improve the process monitoring.

In gas/liquid bubbly flow regime where the acoustic impedance between two medium is high, the use of UT system is more attractable than other methods [10]. The limitation of UT systems in detection of bubbles size in bubbly flow is a problematic issue. Bubble size detection depends mostly on the ultrasonic signal frequencies such that higher frequencies increase the resolution but causes the sensing received signals amplitude to be reduced. Therefore a compromise has to be made between the increasing of frequency and bubble detection size limitation.

Besides hardware limitations, image reconstruction for bubbly flow monitoring by UT systems is still a challenge and need more investigations. The problem arises because of environmental noise, data gathering speed and small number of sensors mounted around the pipes. Therefore a fast and accurate image reconstruction method is necessary in such a case. There are a lot of image reconstruction methods in different areas which have been introduced during the past decades [11-13]. These methods are used to overcome the experimental problems of data collection (different types of sensors have own problem e.g. in X-ray the probabilistic phenomena and or beam hardening of photons or noise in Ultrasonic Systems) or problems during image reconstruction procedures such as artifacts. There are two important types of image reconstruction algorithms: analytical and iterative methods [14]. As a very important member of image reconstruction methods, analytical methods which include linear back projection (LBP), filter back projection (FBP), convolution back projection (CBP), Linogram, filtered Layergram and so on, show their strong ability when a fast reconstruction method is needed (online monitoring e.g. bubbly flow). Therefore in online monitoring where the time consuming is vital, analytical methods have better performance than iterative methods e.g. algebraic reconstruction technique (ART) and simultaneous algebraic reconstruction technique (SART).

In this paper, we concern on analytical methods for transmission mode UT systems in bubbly flow regime. The mathematical theories of analytical methods have been studied briefly, and two common methods i.e. LBP and CBP have been compared on some different bubbly flow phantoms. These phantoms experiments are resembled with real bubbly flow in 2-D structure and allow us to study the performance of different methods in arbitrary selected situations and different sizes. The aim is to find the best filter for fast and accurate image reconstruction.

2.0 THEORY

The mathematical foundation behind all analytical methods for image reconstruction is Radon transform, the inverse Radon transform and projection slice theorem. Figure 1 shows the Radon transform space of a single projection when it passes through an object.

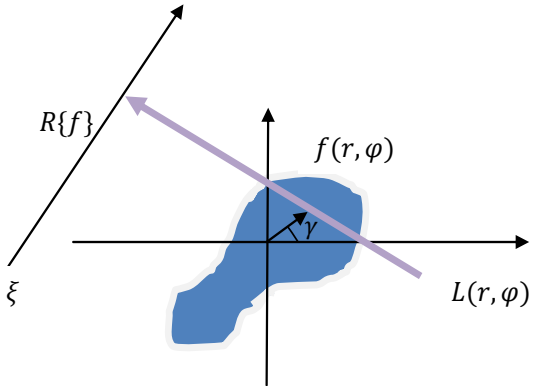

Figure 1 Radon transform of a two dimensional function f(r, φ)

As it is shown in Figure 1a 2-D cross section of an object f(r, φ) mapped to 1-D Radon transform space $R\{f\}$. The following equation shows the mathematic of Radon transform

$$p_\gamma(\xi) = \mathcal{R}\{f\} = \int_{L(r,\varphi)} f(x,y)dL \Rightarrow p_\gamma(\xi) = \int_{-\infty}^{\infty} f(\xi cos(\gamma) - \eta \sin(\gamma), \xi sin(\gamma) + \eta \cos(\gamma))d\eta \quad (1)$$

$p_\gamma(\xi)$ is the attenuated values of all parallel rays which is rotated by γ angle to (ξ, η) coordinate which are given by spatial distribution of f(r, φ).

When all projection values from all angels are collected then an inverse Radon transform is used to reconstruct f(r, φ). The reconstructed object is an approximation of real object because of limitation in the number of projection and angles. The inverse Radon transform is as:

$$f(r,\varphi) = R^{-1}\{p_\gamma(\xi)\} = \frac{1}{2\pi^2}\int_0^\pi \int_{-\infty}^{\infty} \frac{1}{r\cos(\gamma-\varphi)}\, p'_\gamma(\xi)d\eta d\gamma \quad (2)$$

which is a partial differential of p with respect to first variable, a Hilbert transform of it , a back projection of Hilbert transform and finally multiply by $(1/2\pi)$ [14].

2.1 Linear Back Projection

Linear Back Projection (LBP) does not consider the Hilbert transform and partial differentiate of p as it is denoted in Equation (2) and only use back projection operator. The LBP is based on following equation:

$$BP(x,y) = \int_0^\pi p_\gamma(\xi)\, d\gamma \quad (3)$$

The procedure is done by setting all the image pixels along the ray to the same value. The final back projected image is then taken as the sum of all the back projected rays. BP is computationally fast and simple but it is much unsophisticated and the resulting image is very blurry as it is shown in Figure 2.

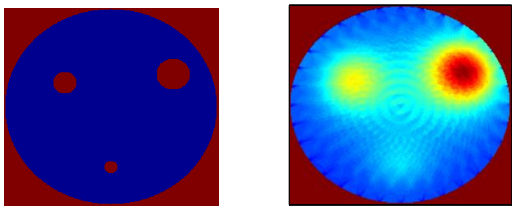

(a) (b)

Figure 2 (a) original image of 3 bubbles in cross section of a pipe (b) blurring image result of Simple Back Projection method

To overcome the blurring image some methods have been introduced.

2.2 2-D Fourier Transform

To achieve f(r, φ) from its projections $p_\gamma(\xi)$, by using Fourier slice theorem in frequency domain we need to calculate the Fourier transform of $p_\gamma(\xi)$ denoted by $P_\gamma(q)$. Then $P_\gamma(q)$ must be rearranging from Polar space to Cartesian space to construct a 2-D Fourier transform of $f(r,\varphi)$ which is called "regridding" [13]. The procedure is shown in Figure 3:

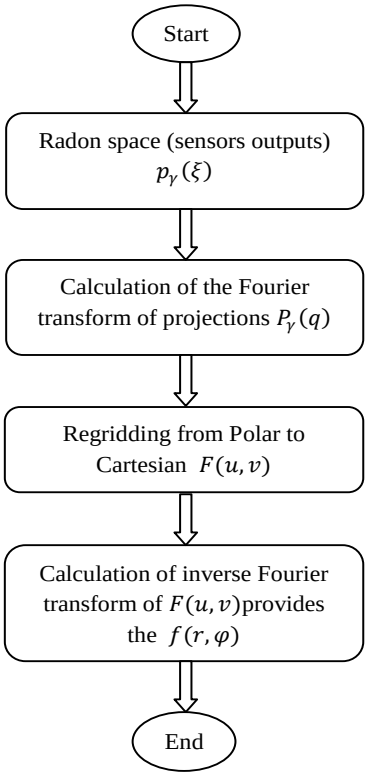

Figure 3 2-D Fourier transform reconstruction method

The interpolation (e.g. bilingual and nearest-neighbor) is needed during the rearrangement of $P_\gamma(q)$ from Polar to Cartesian in Fourier space [15]. This interpolation caused error in high spatial frequencies and decreases the image quality. Moreover the implementation of 2-D Fourier transform is complex and computational.

2.3 Filtered Back Projection

In frequency domain Equation (2) can be written in Cartesian space as:

$$f(x,y) = \int_0^{\pi} \int_{-\infty}^{+\infty} P_\gamma(q) e^{2\pi i q \xi} |q| \, dq d\gamma \quad (4)$$

where $P_\gamma(q)$ is the Fourier transform of $p_\gamma(\xi)$

Let

$$h_\gamma(\xi) = \int_{-\infty}^{+\infty} P_\gamma(q) e^{2\pi i q \xi} |q| dq \quad (5)$$

then

$$f(x,y) = \int_0^{\pi} h_\gamma(\xi) d\gamma \quad (6)$$

Equation (6) is the back projection of $h_\gamma(\xi)$ and Equation (5) is a high pass filter in frequency domain. Unfortunately, $|q|$ is not a square integrable function. Therefore, the mathematical recipe using a convergence-generating regular sequence of functions must be applied. One way is to use windowing and also a high pass filter in frequency domain. Figure 4 shows some of filters e.g. Ram-lak, Hamming and Hanning in a specific window in the frequency domain and time domain.

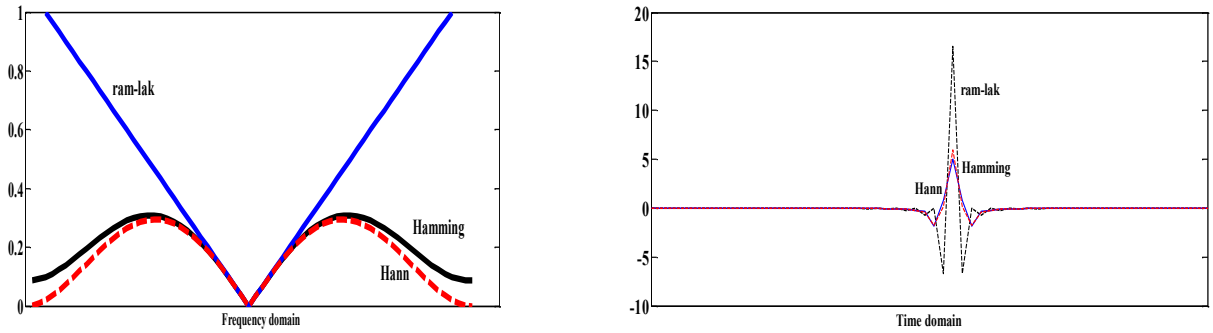

(a) (b)

Figure 4 (a) Ram-Lak, Hamming and Hanning filters in frequency domain (b) Ram-Lak, Hamming and Hanning filters in time domain

2.4 Convolution Back Projection

Equation (5) in time domain is a convolution of two functions and can be written as follows:

$$h_\gamma(\xi) = \int_{-\infty}^{+\infty} p_\gamma(\xi) g(\xi - z) dz \quad (7)$$

where g is the inverse Fourier of $|q|$ (Figure 4a and b).

This time domain version is called convolution back projection (CBP) which is used in all commercial tomography systems. The reason is that the function g can be calculated and saved in a vector and then can be used easily in image reconstruction process.

■3.0 METHODOLOGY

We compare reconstruction images obtained by LBP and CBP in bubbly flow regime. A discrete version of Equation (3) is used to apply LBP to projections values extracted from phantom images. The discrete LBP can be defined as:

$$X = \sum_{i=1}^{N} S_{i,j} . y_j \quad (8)$$

where :

X is the reconstructed image,

S is the sensitivity map from transmitter i to receiver j

y is the value of receiver j

N is the number projection in all angles

Among many types of filters only three filters are selected to apply to the projections values in CBP reconstruction algorithm; Ram-lak, Hanning and Hamming. The Ram-lak filter is a ramp filter with the frequency response of $|q|$ as it is denoted in Equation (5).

Hanning Filter can be written as:

$$w(n) = 0.5(1 - \cos\left(\frac{2\pi n}{N}\right)) \quad 0 < n \leq N \quad (9)$$

where w is the Hanning window, and N+1 is the window length.

Hamming filter can defined as:

$$w(n) = \alpha - \beta \cos\left(\frac{2\pi n}{N}\right) \quad 0 < n \leq N \quad (10)$$

where w is the Hamming window, α, β is the positive constant within the [0,1] interval and N+1 is the window length.

We considered $\alpha = 0.54$ and $\beta = 1 - \alpha = 0.46$ for Hamming filter.

For evaluation of different reconstruction methods in ultrasonic transmission mode, two dimensional phantoms of bubbly flow regime have been simulated using Matlab software. Common projection geometries or sensors arrangement include parallel beam, fan beam and cone beam. Therefore, 32 ultrasonic sensors mounted peripherally around a pipe to form a fan beam configuration of real ultrasonic system in transmission mode. Moreover fan beam data convert to parallel beam to simplify the implementation of CBP.

To measure the quality of reconstructed images, two image assessments were used, peak signal to noise ratio (PSNR) and mean square error (MSE) of reconstruction images. MSE calculated by following formula:

$$MSE = \frac{1}{M^2} \sum (A - B)^2 \quad (11)$$

where A is original phantom, B is reconstructed image and M is the number of rows or columns of images.

PSNR is defined as:

$$PSNR = 10\log(1/MSE) \quad (12)$$

4.0 EXPERIMENTAL RESULTS AND DISCUSSION

Phantom images were simulated using Matlab R2012b to evaluate reconstruction quality of different image reconstruction algorithms. Four image phantoms; an image with four same size bubbles, and three images include three, four and five bubbles with different sizes were simulated as it is shown in Figure 5. The size of phantom images considered as 128*128 pixels as well as reconstructed images. All images consist of two values 0 and 1 for background and bubbles respectively. The image reconstruction procedure contains two parts; forward problem and reconstruction problem. for forward problem a 32 UT sensors with 10 mm length of each sensor, simulated around a circle with 110 mm external radius. The value of each receiver sensor can be calculated as the summation of all pixels values in the path of projections from transmitter to receiver. Each projection has their own sensitivity matrix which includes 0 and 1 value. Figure 6 shows the sensitivity map from transmitter S_4 to receiver S_{23}, typically.

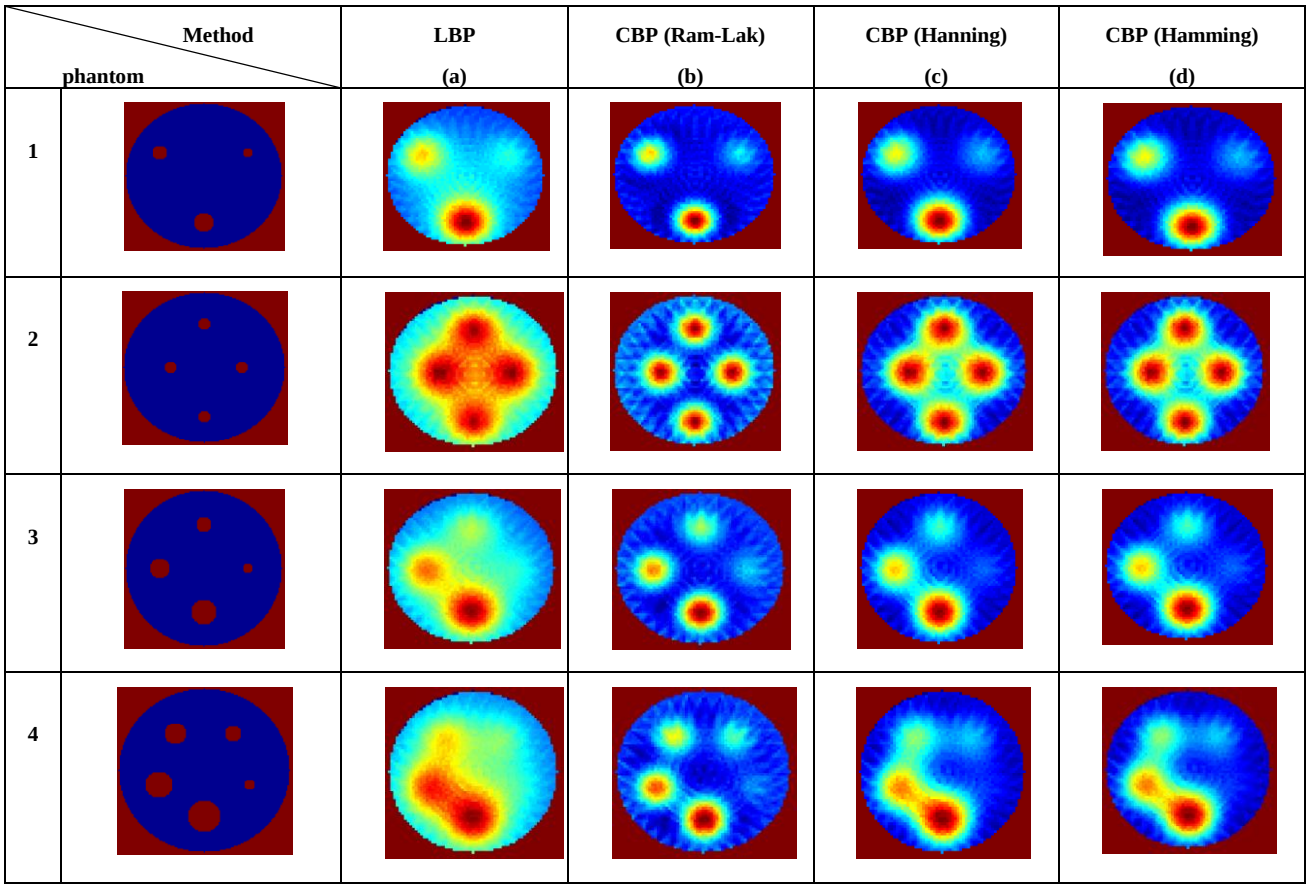

Figure 5 Reconstruction of different bubbles phantom using LBP and CBP (Ram-Lak, Hanning and Hamming). The four images in each column represents reconstruction image from a single method

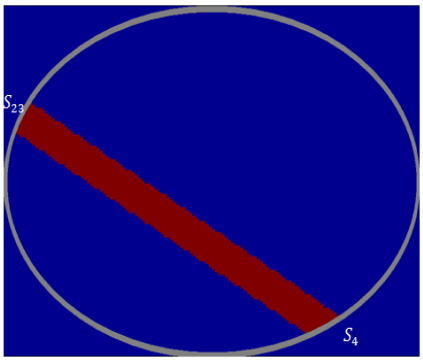

Figure 6 A sensitivity map from sensor S4 to sensor S23

After projection values from all sensors have been calculated the reconstruction procedure based on Equations (4), (8), (9) and (10) is applied. Figure 5 shows the results of reconstruction methods. From Figure 5a it is obvious that LBP cannot reconstruct a high quality image and the results is a blurry image. As it is seen in Figure 5c and d there are not very visually difference between Hanning and Hamming filters while the Ram-Lak filter shows a good performance in such noiseless data. Figure 5b indicates that the performance of Ram-Lak filter is higher than others and in case of same size bubble it has a great visually appearance than others. Figure 5 also shows that when the size of smaller bubble and big bubble in the original image (Figure 5 phantom 4) is very far from each other, small bubble removed in the reconstructed image. Therefore an image processing e.g. adaptive threshold method is needed to detect this small size bubbles.

Figure 7a and b and Table 1 shows the PSNR and MSE results of reconstructed images by different methods. It is obviously clear that in all cases the maximum PSNR belong to Ram-lak filter.

From Figure7b one can see that the maximum MSE belong to LBP method and it is illustrated that the LBP method cannot be a qualify image reconstruction method.

From Table 1 it can be understood that the reconstructed images have a low PSNR even when a Ram-Lak filter is used. In real tomography system, the void fraction is very important and t such reconstructed image cannot be helpful. Therefore in bubbly flow regime where only two materials are combined a threshold method is used to separate gas and liquid from each other in reconstructed image.

Table 1 PSNR and MSE of different reconstructed images

		Phantom1	Phantom 2	Phantom 3	Phantom 4
PSNR	LBP	8.93	5.75	8.185	7.624
	CBP (Ram-Lak)	**10.86**	**9.43**	**10.485**	**10.485**
	CBP(Hanning)	10.26	7.93	9.962	9.518
	CBP(Hamming)	10.35	8.16	10.067	9.637
MSE	LBP	**0.41**	**0.563**	**0.441**	**0.466**
	CBP (Ram-Lak)	0.34	0.39	0.351	0.351
	CBP(Hanning)	0.36	0.453	0.369	0.386
	CBP(Hamming)	0.365	0.442	0.365	0.381

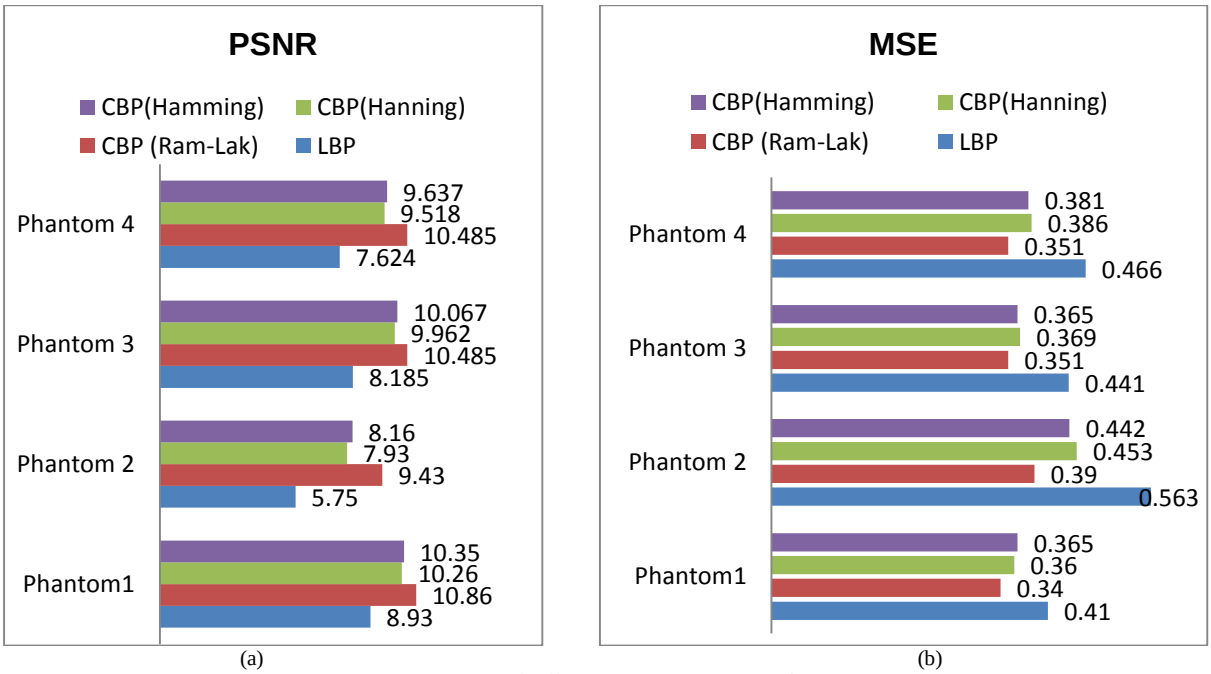

Figure 7 (a) PSNR of different phantoms (b) MSE of phantoms

5.0 CONCLUSION

We have investigated the analytical methods of image reconstruction for online monitoring of bubbly flow regime using ultrasonic transmission mode tomography. Moreover a comparison of reconstructed images quality between LBP and CBP with different filters has conducted. For image quality assessment, two different criteria PSNR and MSE of reconstructed images have used respect to original phantoms which were implemented in Matlab software. The CBP with Ram Lak filter shows superiority to other filters and LBP in terms of PSNR in this study and produced sharper edges bubbles. Therefore CBP with Ram-lak filter is the suitable image reconstruction method for ultrasonic tomography in noiseless conditions.

References

[1] Hoyle, B. 1996. Process Tomography Using Ultrasonic Sensors. *Measurement Science and Technology*. 7(3): 272.
[2] Hoyle, B. 1993. Real-time Ultrasound Process Tomography in Pipelines. In *Ultrasound in the Process Industry, IEE Colloquium on*. IET.
[3] Rahiman, M. H. F., R. A. Rahim, and M. Tajjudin. 2006. Ultrasonic Transmission-mode Tomography Imaging for Liquid/Gas Two-phase Flow. *Sensors Journal, IEEE*. 6(6): 1706–1715.
[4] Rahiman, M. H. F., R. A. Rahim, and N. M. N. Ayob. 2010. The Front-End Hardware Design Issue in Ultrasonic Tomography. *Sensors Journal, IEEE*. 10(7): 1276–1281.
[5] Sazali, Y., *et al*. 2010. *Improving Gas Component Detection of an Ultrasonic Tomography System for Monitoring Liquid/Gas Flow.*
[6] Rahiman, M. H. F., R. A. Rahim, and H. A. Rahim. 2011. Gas Hold-up Profiles Measurement Using Ultrasonic Sensor. *Sensors Journal, IEEE*. 11(2): 460–461.
[7] Nor Ayob, N. M., *et al.* 2013. Design Consideration for Front-End System in Ultrasonic Tomography. *Jurnal Teknologi*. 64(5).

[8] Abbaszadeh, J., *et al.* 2013. Design Procedure of Ultrasonic Tomography System with Steel Pipe Conveyor. *Sensors and Actuators A: Physical*. 203: 215–224.
[9] Pusppanathan. J. *et al.* 2013. *Ultrasonic Tomography Imaging for Liquid-Gas Flow Measurement. Sensors & Transducers*. 148: 33–39.
[10] Manan, M. R., *et al.* 2011. Quantifying Scheme for Detection Heterogeneous Phase in a Pipe Vessel. *International Journal of Research & Reviews in Artificial Intelligence*. 1(1).
[11] Fessler, J. A. 2008. *Image Reconstruction: Algorithms and Analysis*. Under preparation,
[12] Zürner, A., *et al.* 2012. Discrete Tomography of Demanding Samples Based on a Modified SIRT Algorithm. *Ultramicroscopy*. 115: 41–49.
[13] Hsieh, J. 2009. *Computed Tomography: Principles, Design, Artifacts, and Recent Advances*. SPIE Bellingham, WA.
[14] Herman, G. T. 2009. *Fundamentals of Computerized Tomography: Image Reconstruction from Projections*. Springer.
[15] Buzug, T. M. 2008. *Computed Tomography: From Photon Statistics to Modern Cone-beam CT*. Springer.